Estuaries and Coasts (2020) 43:1217–1234
https://doi.org/10.1007/s12237-019-00592-4

SPECIAL ISSUE: IMPACT OF 2017 HURRICANES

Hurricane Irma's Impact on Water Quality and Phytoplankton Communities in Biscayne Bay (Florida, USA)

Anna Wachnicka[1] · Joan Browder[2] · Thomas Jackson[2] · William Louda[3] · Christopher Kelble[4] · Omar Abdelrahman[5] · Erik Stabenau[6] · Christian Avila[5,1]

Received: 28 January 2019 / Revised: 21 May 2019 / Accepted: 4 June 2019 / Published online: 11 July 2019
© Coastal and Estuarine Research Federation 2019

Abstract

The short-term (< 6 months) effects of Hurricane Irma on water quality and phytoplankton community structure were assessed in Biscayne Bay and the adjacent coastal canals from September 2017 through January 2018. The bay experienced sharp fluctuations in daily average salinity and salinity gradients during the passage of the hurricane and significant decreases in salinity as a result of increased freshwater inflows that followed the hurricane (148.2% increase in total inflows in the first week after the hurricane compared to a week before). These decreases were most pronounced in southern and south-central parts of the bay, which experienced the largest post-hurricane increases in freshwater inflows (349.4% and 103.1% in southern and south-central parts of the bay, respectively). Storm-induced increases in inorganic nutrient concentrations stimulated phytoplankton growth in northern, north-central, and southern parts of the bay. Opportunistic phytoplankton taxonomic groups such as chlorophytes and cyanobacteria dominated the total algal biomass pool in the canals, and northern and southern parts of the bay in the weeks following the storm, but they were gradually outcompeted by diatoms in the following months. Changes in spatial-temporal phytoplankton community structure in the months following Hurricane Irma reflect recovery and return to usual seasonal patterns. The effect of Hurricane Irma on water quality and phytoplankton communities was short-lived (< 3 months), suggesting that Biscayne Bay is resilient to tropical cyclones.

Keywords Hurricane · Extreme events · Phytoplankton · Water quality · Biscayne Bay · Nutrients · Salinity distribution · Diatoms · Cyanobacteria · Chlorophytes · Resilience

Communicated by Nancy L. Jackson

Electronic supplementary material The online version of this article (https://doi.org/10.1007/s12237-019-00592-4) contains supplementary material, which is available to authorized users.

✉ Anna Wachnicka
awachnic@sfwmd.gov

Joan Browder
joan.browder@noaa.gov

Thomas Jackson
tom.jackson@noaa.gov

William Louda
blouda@fau.edu

Christopher Kelble
chris.kelble@noaa.gov

Omar Abdelrahman
Omar.Abdelrahman@miamidade.gov

Erik Stabenau
erik_stabenau@nps.gov

Christian Avila
Christian.Avila@miamidade.gov

[1] Coastal Ecosystems Section, South Florida Water Management District, 3301 Gun Club Rd, West Palm Beach, FL 33406, USA

[2] National Oceanic and Atmospheric Administration, Miami, FL 33149, USA

[3] Florida Atlantic University, Boca Raton, FL 33431, USA

[4] Atlantic Oceanographic and Meteorological Laboratory, National Oceanic and Atmospheric Administration, Miami, FL 33149, USA

[5] Miami-Dade County Department of Environmental Resources Management, Miami, FL 33136, USA

[6] South Florida Natural Resources Center, National Park Service, Homestead, FL 33030, USA

Introduction

Hurricanes impact estuaries by drastically changing their geomorphology, biogeochemistry, and habitats (Zhang et al. 2005; Mallin and Corbett 2006; Paerl et al. 2018). Increased freshwater inflows and precipitation during and just after hurricanes cause sudden changes in inshore water-column salinity, temperature, transparency, and dissolved oxygen concentration (Mallin et al. 1999; Paerl et al. 2006; Hagy et al. 2006; Steward et al. 2006), while winds cause strong wave action that degrades benthic habitats (Woodley et al. 1981; Wilson et al. (this volume)). Hurricane-induced internal and external nutrient loads often lead to phytoplankton blooms and shifts in the phytoplankton community composition (Hagy et al. 2006; Zhao et al. 2008; Liu et al. 2009; Paerl et al. 2001, 2006, 2018). Increased influx of terrigenous organic material and resuspension of estuary sediments increase biochemical oxygen demand, often resulting in hypoxia (Mallin et al. 1999; Tomasko et al. 2006; Bianucci et al. 2018). These cascading ecological and physicochemical impacts ultimately affect higher food-web trophic levels (Stevens et al. 2006; Munroe et al. 2013; Strickland et al. (This volume); Massie et al. (this volume); Zink et al. (this volume)).

Hurricane Irma was a category 4 storm with 213-km/h maximum sustained winds (the highest 1-min average wind speeds measured at the standard meteorological height of 10 m in an unobstructed exposure (Powell et al. 1996)) when it made landfall in the Florida Keys on September 10, 2017 (Cangialosi et al. 2018). Tropical-storm force winds (63–117 km/h) extended outward up to 650 km from the hurricane's center and wind gusts reached over 126 km/h along southeast Florida coast (Cangialosi et al. 2018). Biscayne Bay, located outside of the eye wall in the strong northeast quadrant of the storm, was exposed to 86–108-km/h winds and a 1.2–1.8-m storm surge (Cangialosi et al. 2018). The combined effects of storm surge and high tide produced coastal inundation of 1–3 m aboveground along the bay (South Florida Water Management District 2018a). As the storm moved over the area, strong winds caused extensive damage to coastal mangroves (Radabaugh et al. (2019)), estuarine mangrove islands (Wingard et al. (this volume)), and urban infrastructure, including local sewage treatment plants, which released millions of liters of raw and partially treated wastewater into the bay during power outages (Florida Department of Environmental Protection 2018).

Due to the sampling constraints directly after tropical cyclones, little is known about the immediate-, short-, and long-term impacts these weather systems have on water quality in South Florida estuaries. The goal of this study was to evaluate the short-term effects of Hurricane Irma on Biscayne Bay water quality and phytoplankton communities. Detailed water quality and phytoplankton community structure analyses were performed on data collected from the coastal canals and inshore locations of the bay for 6 months after the hurricane, and an overview of pre- and post-hurricane water quality conditions was provided for the entire bay based on data collected from offshore locations and the northern part of the bay.

Methods

Study Area and Sampling Locations

Biscayne Bay is a large (~ 700 km^2), shallow (~ 2-m avg. water depth), subtropical, lagoonal estuary with a mixed urban-agricultural watershed (2429 km^2; Fig. 1a,b; Carey et al. 2011). The coastal area adjacent to the northern part of Biscayne Bay is the metropolitan area of Miami, while south-central and southern parts of the bay are farmlands and coastal wetlands (Fig. 1a,b; Carey et al. 2011). These differences in the watershed result in different nutrient loadings to the bay, with elevated nitrate-nitrite (NO_x) loads from southern agricultural areas into southern Biscayne Bay and elevated ammonium (NH_4^+) and phosphate (PO_4^{3-}) loads from urban areas into northern Biscayne Bay (Caccia and Boyer 2005, 2007; Carey et al. 2011; Briceño et al. 2013). The exchange of water between the Atlantic Ocean and the bay occurs through the "Safety Valve" (central main opening to the bay) and the tidal creeks between the barrier islands. Freshwater enters the bay via the coastal drainage canals and natural creeks, precipitation, and groundwater (Langevin 2003; Stalker et al. 2009). Salinity remains > 30 PSU in the entire bay area during dry seasons (November 1–April 30) and drops to < 10 near canals and creeks during wet seasons (May 1–October 30; Briceño et al. 2013).

Water quality and phytoplankton samples were collected from 12 inshore (north-south transect) and 20 canal (east-west transects) sites by the South Florida Water Management District (SFWMD) and National Oceanic and Atmospheric Administration (NOAA) team on a bi-monthly basis, between September 2017 and January 2018 (Fig. 1a). Additional monthly water quality data from 18 offshore locations monitored by Miami-Dade Department of Environmental Resource Management (DERM) and daily average salinity data from 20 bottom recorders maintained at inshore locations by Biscayne National Park (BNP) were used in this study (Fig. 1b). All transects encompass the gradient of salinity and nutrients characterizing the bay coastal zone.

Atmospheric and Flow Data

Radar-based daily rainfall data from Biscayne Bay were obtained from the Next Generation Radar (NEXRAD; NEXRAD 2018). Daily wind, sea surface temperature (SST), and air temperature (Air T) data were obtained from the NOAA National Weather Service Virginia Key

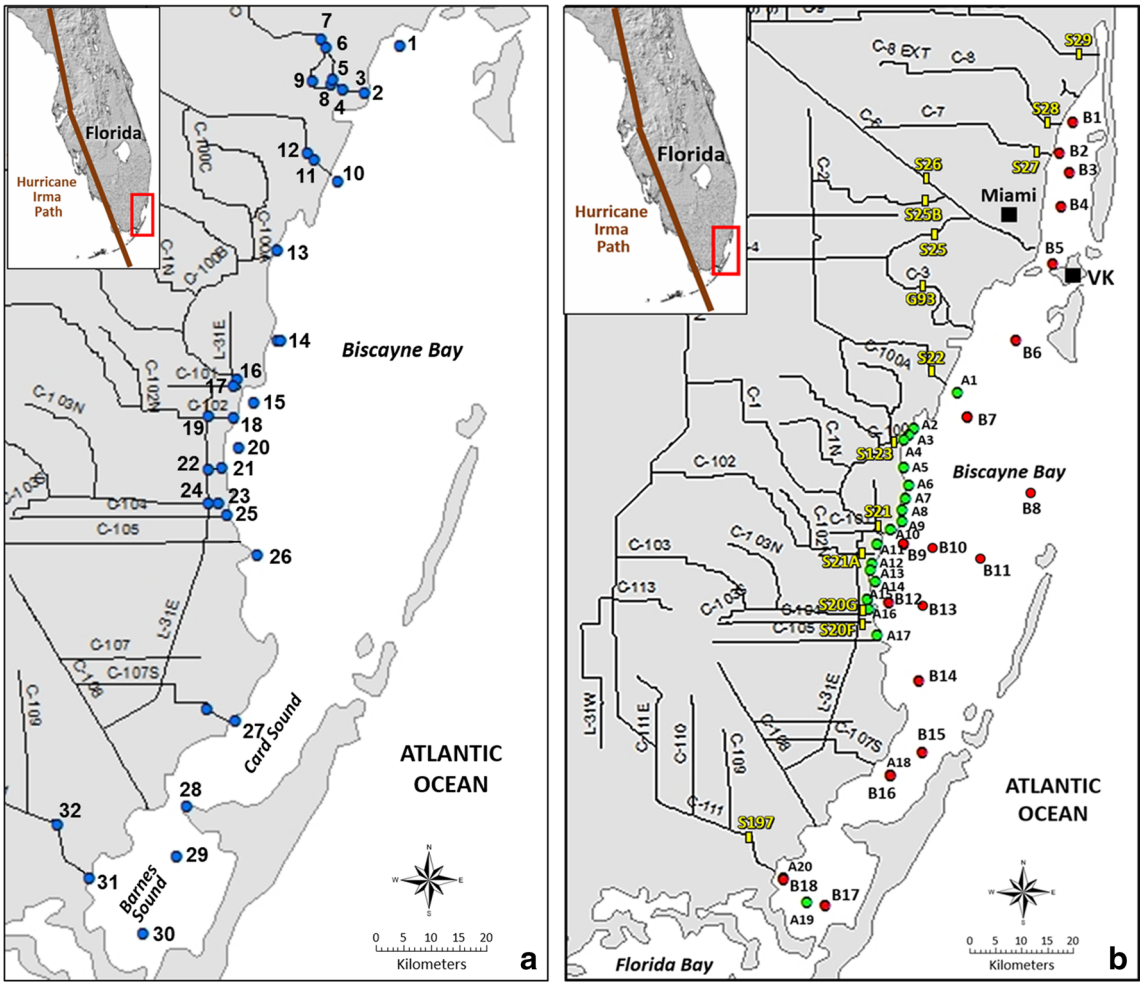

Fig. 1 Map showing the locations of sampling sites in Biscayne Bay used for this study: **a** 32 SFWMD/NOAA sites (blue dots), and **b** 20 selected BNP sites with data recorders (green dots) and 18 selected monthly DERM monitoring sites (red dots). Yellow rectangles indicate the location of the SFWMD coastal structures. VK = NOAA Virginia Key Meteorological Station

meteorological station in Miami, Florida (Figs. 1a and 2; NOAA 2018).

Total daily discharges into Biscayne Bay were estimated based on the flow data from the 14 major SFWMD-operated structures on Snake Creek (S-29/C9), Biscayne (S-28/C8), Little River (S-27/C7), Miami North (S-26/C6), Tamiami (S-25B/C4), South Fork Miami River (S-25/C5), Coral Gables (G-93/C3), Snapper Creek (S-22/C2), Cutler Drain (S-123/C100), Black Creek (S-21/C1), Princeton (S-21A/C102), Military (S-20G/G95), Mowry (S-20F/C103), and Aerojet (S-197/C111) canals (Figs. 1a,b and 2b; South Florida Water Management District 2015; 2018a). The daily flow values were used to calculate total annual and monthly inflows into Biscayne Bay.

Field and Lab Methods

Physical water quality data (salinity (S), temperature (T), turbidity (Turb), dissolved oxygen (O_2), pH) were recorded at each SFWMD/NOAA, DERM, and BNP location using YSI 6600 sondes. Fifty-five milliliters of water was collected from each location and filtered through 0.45-μm Whatman PTFE syringe filters in the field and placed in coolers on ice for the duration of each sampling trip. In the lab, samples were stored frozen until ready for inorganic nutrient (silica (SiO_2), nitrate (NO_3^-), nitrite (NO_2^-), NH_4^+, PO_4^{3-}) analyses. All analyses were performed according to the standard United States Environmental Protection Agency (US EPA) procedures (EPA SM4500F, 353.2, 350.1, 365.1) at the NOAA Atlantic Oceanographic and Meteorological Laboratory (NOAA AOML) in Miami, FL.

An additional 3000 ml of water was collected at each SFWMD/NOAA site for pigment-based chemotaxonomic analyses of total and phytoplankton class-specific biomass (chlorophylls and carotenoids) and relative abundance of major phytoplankton classes (diatoms, dinoflagellates, cyanobacteria, chlorophytes, and cryptophytes). Sampled water was stored in Nalgene amber bottles and placed in coolers

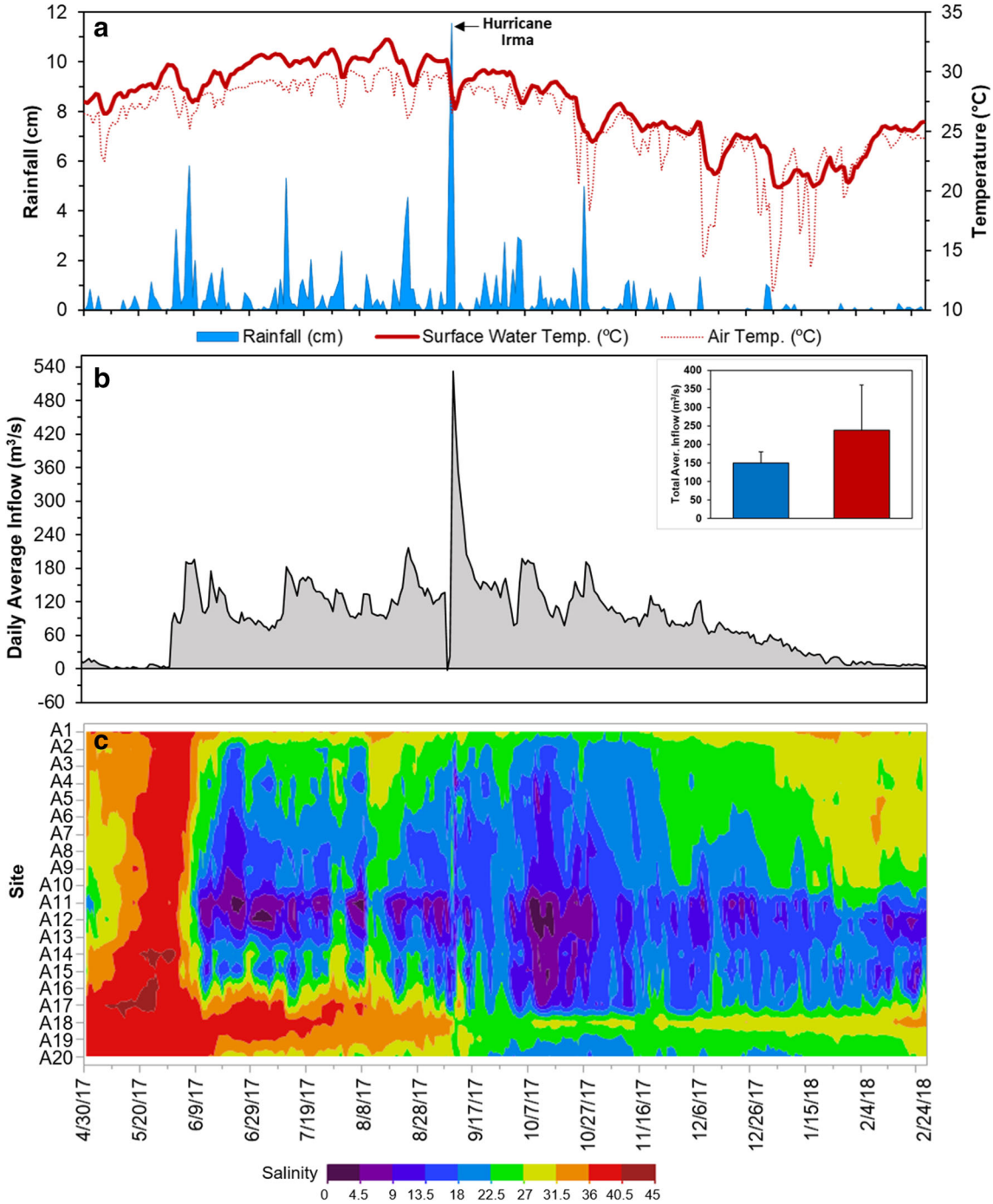

Fig. 2 **a** Temporal variation in daily rainfall (cm) across Miami-Dade County, and daily surface water and air temperature (°C) at Virginia Key Meteorological Station (Key Biscayne, Florida). **b** Total daily average inflows from 14 canal structures into Biscayne Bay, and difference in total average inflows into the bay 2 weeks before (blue) and after (red) Hurricane Irma (chart in the upper right corner). **c** Daily average bottom salinity (PSU) at 20 inshore locations Biscayne Bay (north (top) to south (bottom) transect)

on ice for the duration of each sampling trip to protect the pigments from photodegradation and disintegration. Between 1000 and 3000 ml of water was filtered through GF/F glass microfiber filters (nominal pore size 0.7 μm and 47 mm diameter) using a vacuum pump (< 5 in Hg) immediately after arrival in the lab. Filtered samples were stored at − 80 °C until ready for analyses. Photosynthetic (chlorophylls) and photoprotective (carotenoids) pigments were extracted following Hagerthey et al. (2006), separated and identified using Reversed Phase High-Performance Liquid Chromatography (RP-HPLC) with a ternary gradient including ion-pairing reagents (Louda et al. 1998), and quantified by

the Beer-Lambert Law relationship using the integrated peak areas at appropriate wavelengths in the Environmental Biogeochemistry Lab at Florida Atlantic University (FAU). Taxon-specific algal biomass (chl *a*) was estimated using chl *a*/marker pigment ratios determined by multiple regression/multiple simultaneous equation formulae (Grant and Louda 2010). Samples for nutrient and chemotaxonomic analyses were collected at 0.3-m water depth below the surface, and physical water quality measurements were taken at 0.3 m below the surface and 0.3 m above the bottom.

Statistical Methods

Environmental data were checked for outliers, square-root transformed, and standardized via z scores to more closely approximate a normal distribution and to equalize variable distribution to a common scale (McCune et al. 2002). The improvement of normality was checked by evaluating values of skewness and kurtosis for each variable before and after transformation. Principal component analysis (PCA) was used to visualize similarities in water quality among locations and to describe different sources of variation in water quality among sites (Jolliffe 2011). Similarity in water quality among sites was determined using hierarchical clustering with Euclidean distance measure and group average linkage method and visualized in two-dimensional PCA ordination diagrams (Kruskal and Wish 1978).

Compositional similarity in phytoplankton community structure was determined using hierarchical clustering with Sørensen distance measure (Bray and Curtis 1957) and flexible beta ($\beta = -0.25$) linkage method (McCune et al. 2002) and was visualized in nonmetric multidimensional (NMDS) ordination diagrams (Kruskal and Wish 1978). Explanatory water quality variables were overlain as "vectors" representing the direction and strength of the plane of the maximum correlation with phytoplankton community similarity. Stress statistics were used as a measure of distortion in the ordination diagram. Indicator species analysis (ISA) was used to identify the phytoplankton classes, which were the most abundant and most frequently occurring at each location (canals vs. inshore) and clusters during each sampling event. The indicator value (IV_{kj}; a value of 100 represents the best indicator of a particular group) was calculated by multiplying the value of proportional abundance of each class in a designated group relative to the abundance of that class in all groups by the proportional frequency of the same class in each group (Dufrêne and Legendre 1997; McCune et al. 2002).

The statistical significance of differences in water quality and phytoplankton community structure among locations (canals vs. inshore), sampling events, and clusters was tested with a Permutational Multivariate Analysis of Variance (PERMANOVA), a nonparametric multivariate statistical test (Anderson 2001, 2014). The Kruskal-Wallis test (Kruskal and Wallis 1952), a rank-based nonparametric test, was used to determine if the median concentrations of different water quality variables differed among clusters, while the Dunn-Bonferroni post hoc test (Dunn 1964) was used to make all possible cluster pairwise comparisons. The Similarity Percentage (SIMPER) analysis was used to determine the percentage contribution of different phytoplankton classes and water quality variables to the separation of the groups (locations, clusters; Clarke 1993). RELATE, a nonparametric type of Mantel test, was used to test how well the patterns in biological data matched those in environmental data (the closer the ρ values were to 1, the more similar the patterns in biological and environmental data were; Clarke et al. 2014). The BIO-ENV procedure was used to find sets of environmental variables that best explained the patterns in biological communities, and distance-based linear modeling (DistLM) was used to determine how much of the variation in biota can be explained by environmental variables (Clarke et al. 2014). A marginal test, a nonparametric significance test, was used to determine how much variation in biological data each environmental variable can explain. The sequential test, a conditional test of individual variables, was used to examine whether adding particular variables contributed significantly to the explained variation in biological data. Akaike's information criterion (AICc), which measures the relative quality of a statistical model for a given set of data, was used to select the best model with environmental variables that explain most of the variation in the phytoplankton community structure (Clarke et al. 2014). The strength and direction of association among water quality and algal biomass variables were assessed with Spearman rank correlation analysis, and the significance of the results were assessed using the t test. All analyses were conducted using Statistical Package for Social Sciences (SPSS) version 25, John's Macintosh Project (JMP) version 14, Personal Computer-Ordinations (PC-Ord) version 6, and Plymouth Routines in Multivariate Ecological Research (Primer) version 7 (Clarke and Gorley 2015) .

Results

Atmospheric Conditions

Total average daily precipitation reached a record of 11.5 cm across Miami Dade County on September 10, which represented 36.4% of the total September precipitation (31.6 cm; NEXRAD 2018; Fig. 2a). Total September precipitation was 32.8% higher than the SFWMD 30-year average (1986–2015) rainfall for this month (21.2 cm) in Miami Dade County (South Florida Water Management District 2018b). The maximum wind speed recorded during the passage of Hurricane Irma at the Virginia Key meteorological station (Key Biscayne, FL) was 85.3 km/h with wind gusts up to

114.5 km/h (67 km/h and 89.6 km/h daily average wind speed and maximum gusts, respectively; NOAA 2018). Wind speed during the event increased by approximately 800% compared to the week before the hurricane (10.8–16.2 km/h weekly average wind speed and maximum gusts). SST dropped by ~3 °C from an average of 30.4 °C a week prior to the event (NOAA 2018; Fig. 2a). Air T also dropped after the hurricane by an average of ~1 °C (Fig. 2a).

Freshwater Inflows

The 2017 total annual inflow from the 14 major coastal structures into inshore regions of Biscayne Bay (27,649.4 m^3/s) was the largest in the last decade and 26% larger than the year before (22,009.1 m^3/s; South Florida Water Management District 2018a). Total monthly discharges increased by 34% in September compared to August (5288.8 m^3/s vs. 3938.4 m^3/s, respectively) and by 78% in the 2-week period after the storm compared to the same period before the event (3344.5 m^3/s vs. 1876.7 m^3/s, respectively; Fig. 2b). Maximum daily discharges occurred a day after the hurricane, on September 11 (532.4 m^3/s). Most of the water that entered Biscayne Bay was discharged into central and southern Biscayne Bay both 2 weeks before and 2 weeks after Hurricane Irma. The largest 2-week post-hurricane increase in total inflows occurred from Military Canal (G-95/S-20G; 716.3% increase from the 0.4-m^3/s 2-week average inflow prior to the hurricane) and Cutler Drain Canal (C-100/S-123; 356.0% increase from the 4.0-m^3/s 2-week average inflow prior to the hurricane) into the central part of the bay, and Aerojet Canal (C-111/S-197; 349.4% increase from the 9.8-m^3/s 2-week average inflow prior to the hurricane) into Manatee Bay (Fig. 3). The largest post-hurricane average daily discharges were recorded from the Aerojet Canal (C111/S-197; aver. 43.9 ± 15.8 m^3/s), Snake Creek Canal (C9/S-29; 33.1 ± 12.3 m^3/s), and Mowry Canal (C103/S-20F; 30.5 ± 23.1 m^3/s; Fig. 3). Both the magnitude and variation in daily average discharges increased in most of the canals after the hurricane (except for Miami North Fork (C6/S-26) and Tamiami (C4/S-25B) canals; Fig. 3). The 2017 wet season discharges were significantly higher during increased periods of precipitation ($\rho = 0.402$; $p = 0.000$; Fig. 2a,b).

Water Quality

Significant temporal ($F = 16.600$, $p = 0.001$) and spatial ($F = 6.213$, $F = 13.662$, and $F = 10.234$ at $p = 0.001$ in September and November 2017, and January 2018, respectively) differences in water quality were present at the sampling locations after the hurricane (Figs. 2c and 4a–d; Table 1). Daily bottom S was significantly lower during higher freshwater inflows ($\rho = -0.489$; Fig. 2b, c). In general, nutrient concentrations and T decreased with increasing distance from the canal structures towards the inshore locations (except for September when T was lower in the canals compared to the inshore locations), while S and O_2 increased (Fig. 5a–c; Table 2). On average, O_2 levels were lower in September compared to November and January and in the canals compared to inshore sites (Fig. 5a–c). The lowest September O_2 concentrations were recorded in Snapper Creek (C2), Coral Gables (C3),

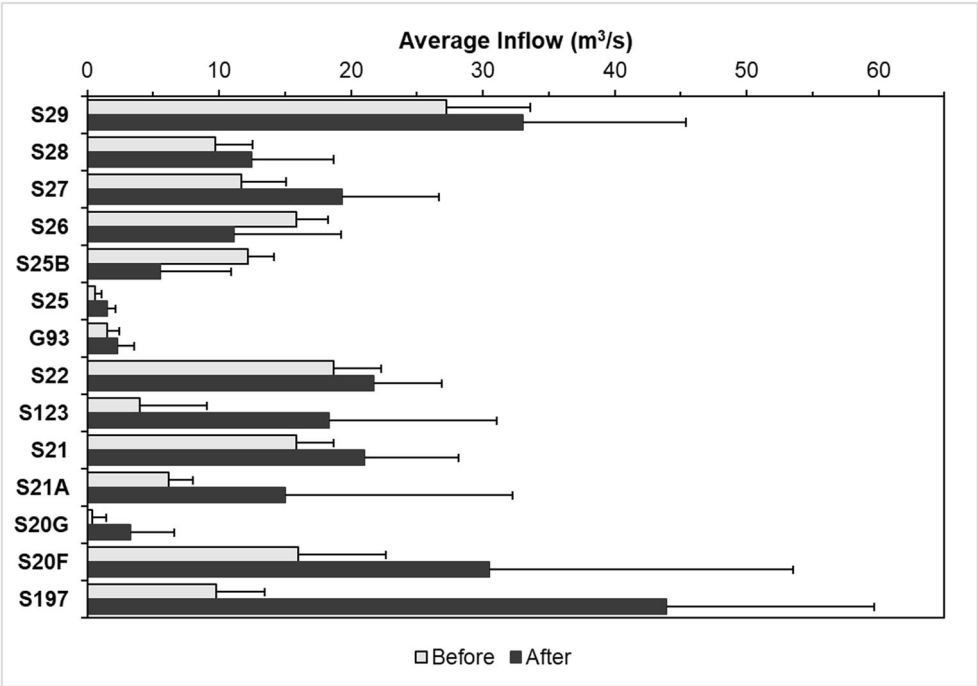

Fig. 3 Average discharges from 14 major coastal canal structures (coastal structure IDs on the *Y* axis) into Biscayne Bay 2 weeks before (gray bars) and after (black bars) Hurricane Irma

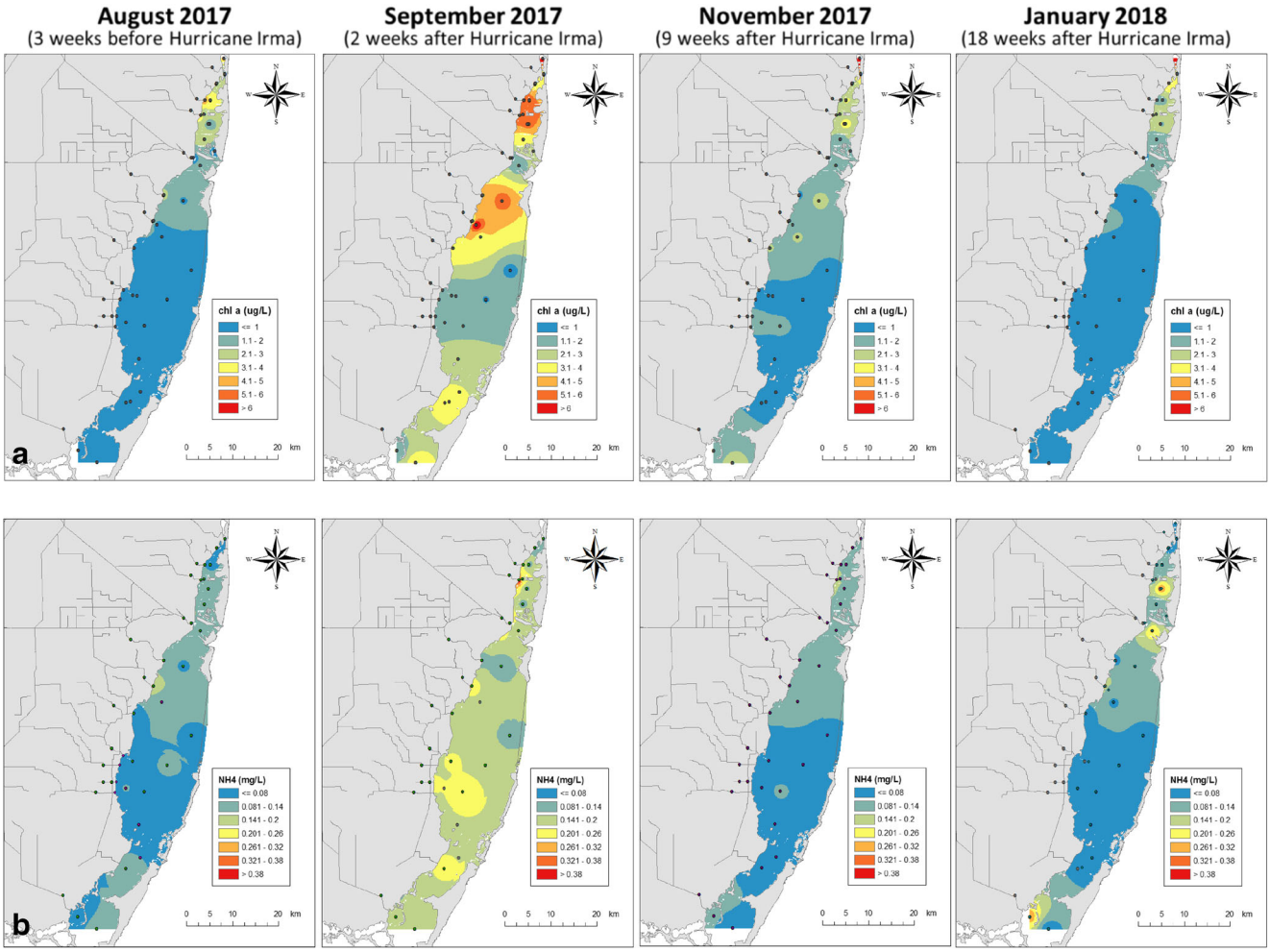

Fig. 4 Spatial and temporal differences in chl a (μg/l), ammonia (NH4) (mg/l), nitrate and nitrite (NO_x) (mg/l), and orthophosphate (PO_4) (mg/l) across Biscayne Bay during August, September, and November 2017, and January 2018 surveys. Black dots represent DERM monitoring locations and pink dots represent SFWMD/NOAA monitoring locations

and Gould canals (C1; < 2–3 mg/l). Water column stratification was recorded at many inshore locations.

PCA analysis revealed that most of the variation in water quality could be explained by the first two principal components (PC1 and PC2; 54.3%, 61.0%, and 63.8% of the total variation explained in September, November, and January, respectively; Fig. 5a–c; Table 3). In September, the marine inshore locations in the southernmost and northernmost parts of the bay (cluster D) were significantly warmer compared to the north fork of the Coral Gables Canal (C3; cluster A) as well as at other canals and inshore locations (cluster E; $p < 0.05$; Fig. 5a). On the contrary, the canals were more nutrient-enriched (north fork of the Coral Gables Canal (cluster A) in NO_2^-, lower part of the Coral Gables Canal (cluster C) in NO_3^-, and other canals and the remaining inshore locations (cluster E) in SiO_2) than the inshore locations (cluster D; $p < 0.05$; Fig. 5a). The lower part of the Coral Gables Canal (cluster C) had also a significantly higher concentration of PO_4^{3-} than the other canals and inshore sites in the central part of the bay (cluster E; $p < 0.05$; Fig. 5a).

In November, most of the canal sites (cluster E) were significantly warmer and less oxygenated compared to the inshore locations (cluster D; Fig. 5b). They had also higher nutrient concentrations (NO_3^- in Princeton Canal (C102; cluster C), NH_4^+ in the north fork of the Coral Gables Canal (C3; cluster A), and PO_4^{3-} in the other canals (cluster E)) relative to the inshore locations (cluster D; $p < 0.05$; Fig. 5b).

In January, water in the south fork of the Coral Gables Canal (C3; cluster E) was significantly warmer than at any inshore location, the lower part of the Coral Gables Canal, or the Snapper Creek Canal (C2; cluster B; $p < 0.05$; Fig. 5c). Princeton (C102) and Mowry (C103) canals (cluster D), and the north fork of the Coral Gables Canal (cluster E) had significantly higher SiO_2 and NO_3^-, and NO_2^- (only Princeton and Mowry canals) than the inshore locations, and the lower part of the Coral Gables Canal (C3) and Snapper

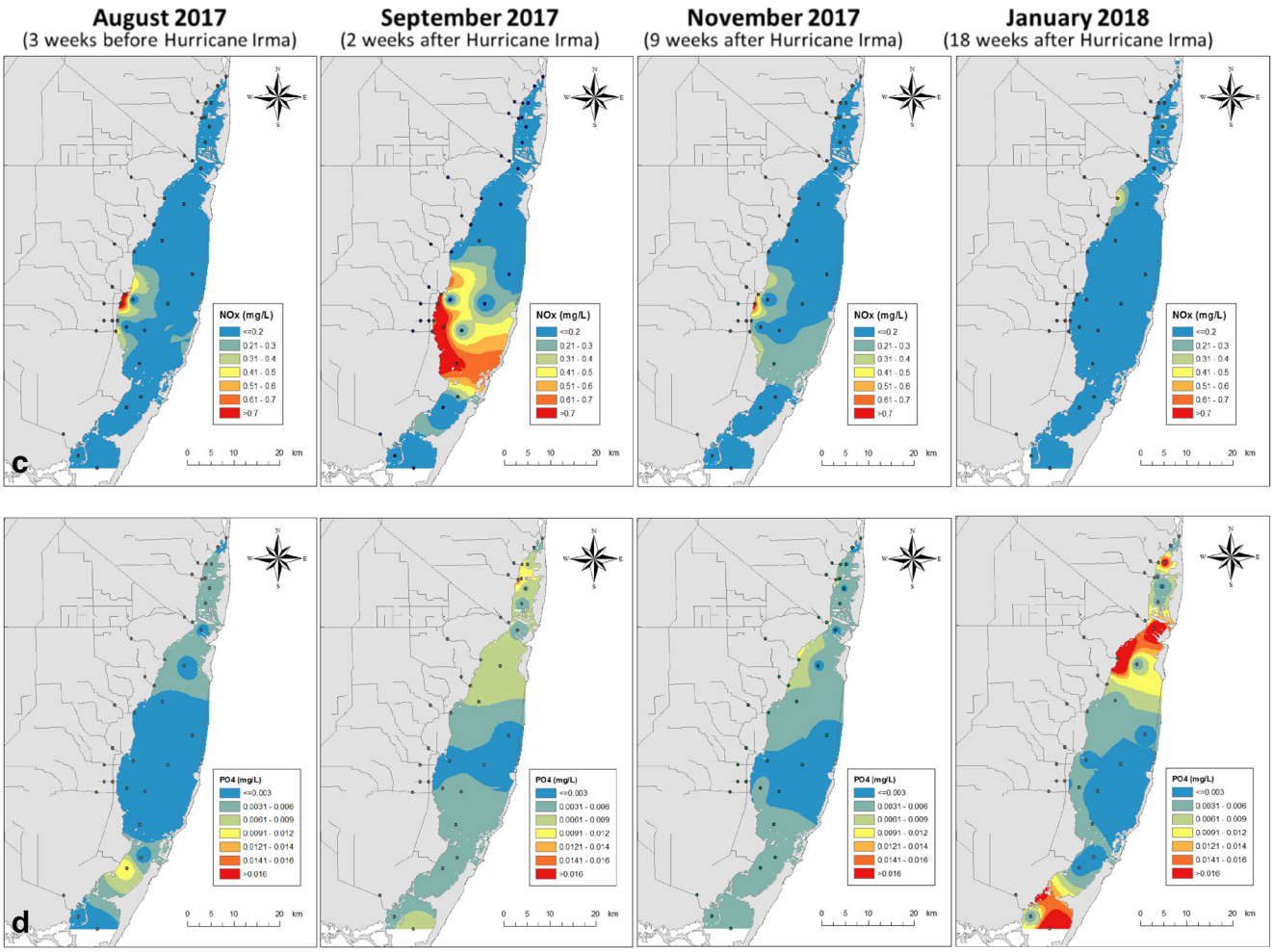

Fig. 4 (continued)

Creek Canal (C2; cluster B; $p < 0.05$; Fig. 5c). NH_4^+ was significantly higher in Aerojet (C111), Black Creek/Gould (C1), and Military (G95) canals (cluster C) compared to any inshore location, lower part of the Coral Gables Canal, or Snapper Creek Canal (cluster B; $p < 0.05$). PO_4^{3-} was significantly higher in the north fork of the Coral Gables Canal (cluster E) compared to the lower part of the Coral Gables Canal and Snapper Creek Canal (cluster B), and Mowry and Princeton canals (cluster D; $p < 0.05$; Fig. 5c).

Spatial and Temporal Distribution Patterns of Phytoplankton Communities

Compared to the 2016 dry season (mid-December), the abundances of chlorophytes, cryptophytes, and dinoflagellates were significantly higher in the 2018 dry season (early January; $p < 0.05$; Fig. 6a, b). Algal biomass, expressed as chlorophyll *a* (chl *a*) concentration, was significantly higher in September compared to November and January ($p < 0.05$; Figs. 4a and 6c). The September biomass was also significantly higher at inshore locations compared to the canals ($p < 0.05$; Fig. 6c). Overall, chl *a* was highest in northern (1.1–6.1 μg/l) and southern (1.2–3.6 μg/l) parts of the bay compared to the central part (Figs. 4a, 6d, and 9). Biomass in these two regions significantly increased in September compared to the months before the hurricane ($p < 0.05$) and then gradually declined to pre-hurricane levels in the following months (Fig. 6 d).

The phytoplankton community structure differed significantly among post-hurricane sampling events ($F = 8.908$, $p = 0.001$), and these differences were captured in the 2-dimensional NMDS ordination diagrams (Fig. 7a–c). Pairwise tests found September communities to be significantly different from November ($t = 3.012$, $p = 0.001$) and January ($t = 4.198$, $p = 0.001$) communities, but November and January communities were comparable ($t = 1.506$, $p = 0.089$; Fig. 7a–c). Much of the differences in community structure among sampling events was driven by the presence of diatoms and cyanobacteria, which contributed 30.1% and 26.1%, respectively, of the total difference between the September and

Table 1 Summary statistics of surface water quality parameters (chlorophyll a (chl A) (μg/l), ammonium (NH_4^+) (μM), nitrite (NO_2^-) μM, nitrate (NO_3^-) μM, O_2 = dissolved oxygen (mg/l), orthophosphate (PO_4^{3-}) (μM), salinity (PSU), silica (SiO_2) (μM), temperature (°C), Turb = turbidity (NTU)) at all sampling sites recorded during three post–Hurricane Irma surveys in Biscayne Bay

Variables	Number	Range	MN	MAX	Mean	SD
September, 2017						
chlA	32	4.5	0.00	4.46	1.16	1.03
NH_4^+	32	37.8	0.59	38.40	13.85	7.88
NO_2^-	32	2.6	0.05	2.64	0.95	0.67
NO_3^-	32	106.5	1.22	107.75	33.30	33.16
O_2	32	6.1	1.11	7.21	4.29	1.55
pH	32	0.8	7.07	7.66	7.47	0.21
PO_4^{3-}	32	1.6	0.00	1.61	0.15	0.37
S	32	29.9	0.27	30.13	11.64	10.03
SiO_2	32	168.0	7.92	175.88	73.93	44.34
Temp	32	4.4	27.84	32.28	29.64	1.08
Turb	32	6.3	0.00	6.30	1.07	1.39
November, 2017						
chlA	32	1.4	0.21	1.63	0.62	0.35
NH_4^+	32	50.0	0.59	50.57	7.95	10.39
NO_2^-	32	2.6	0.18	2.75	0.72	0.58
NO_3^-	32	184.5	1.19	185.71	29.94	43.22
O^2	32	6.0	2.63	8.58	5.55	1.66
pH	32	0.9	7.35	8.21	7.89	0.23
PO_4^{3-}	32	1.2	0.00	1.19	0.15	0.34
S	32	30.5	0.29	30.82	14.72	0.09
SiO_2	32	178.1	1.95	180.01	63.06	50.33
Temp	32	3.1	23.52	26.55	24.87	0.78
Turb	32	4.2	0.00	4.20	0.80	0.86
January, 2018						
chlA	32	3.3	011	3.40	0.66	0.68
NH_4^+	32	22.8	0.00	22.76	3.44	4.63
NO_2^-	32	1.0	0.02	0.98	0.36	0.25
NO_3^-	32	190.1	0.06	190.20	20.79	45.76
O_2	32	6.8	2.29	9.04	6.81	1.38
pH	32	1.7	6.75	8.41	7.95	0.35
PO_4^{3-}	32	1.3	0.00	1.30	0.15	0.34
S	32	27.0	5.85	32.90	21.50	7.64
SiO_2	32	103.1	1.05	104.17	36.42	32.25
Temp	32	7.1	15.51	22.65	19.57	1.84
Turb	32	6.9	0.10	7.00	1.97	1.57

November community structure, and 24.3% and 28.1%, respectively, of the total difference between the September and January community structure (Fig. 7a–c). Canal and inshore communities differed significantly in September and November ($t = 2.372$, $p = 0.002$ and $t = 1.879$, $p = 0.027$, respectively; Fig. 7a–c). Cyanobacteria and dinoflagellates were more frequently found and at higher abundance at inshore sites (62.3% IV; $p = 0.037$ and 64.0% IV, $p = 0.025$, respectively), while chlorophytes were more common in the canals (66.9%, $p = 0.002$ IV; Fig. 7a–c). The phytoplankton community structure differed significantly among groups defined by cluster analysis in all three sampling events ($p < 0.05$; Fig. 7a–c).

Spatial patterns in phytoplankton communities and water quality were different in September and January ($p > 0.05$), but similar in November ($\rho = 0.282$, $p = 0.014$). Water quality variables that best explained phytoplankton community patterns in September were S and PO_4^{3-} (35.4% of variation explained ($R^2 = 0.354$; Fig. 7a). S, T, and NO_2^- best explained phytoplankton community patterns in November (46.1% of variation in their structure ($R^2 = 0.461$) and 34%, 6.9%, and 5.2% contribution, respectively; Fig. 7b). Temperature best explained phytoplankton community patterns in January (12.1% of variation explained ($R^2 = 0.121$; Fig. 7c).

In September, cyanobacteria were frequently found and had high abundance at marine sites with elevated NH_4^+ concentrations south of Convoy Point, in Card Sound and Barnes Sound, and in North-Central Biscayne Bay (cluster E; 35.5% IV, $p = 0.0004$), while dinoflagellates were associated with the more turbid sites in Military Canal (G95) and Barnes Sound (cluster F; 60.5% IV, $p = 0.001$; Figs. 7a, 8, and 9). Cryptophytes were frequently recorded and abundant at freshwater sites with elevated NO_x and SiO_2 in Coral Gables (C3), Princeton (C102), and Snapper Creek (C2) canals (cluster B; 45% IV, $p = 0.0002$), while diatoms were higher in Aerojet Canal (C111) and at inshore locations north of Black Creek (c1) Canal (cluster A; 30.8% IV, $p = 0.0214$; Fig. 7a). In November, cyanobacteria were still abundant in Barnes Sound and Card Sound (cluster C and A; 62.3% IV, $p = 0.0002$), while chlorophytes increased in nutrient-enriched waters of Coral Gables (C3) and Snapper Creek (C2) canals (cluster B; 74.3% IV, $p = 0.0002$; Figs. 7b). In January, chlorophytes remained abundant in warmer and nutrient-enriched waters of Coral Gables (C3) and Military (G95) canals and at inshore sites in North-Central Bay (cluster A; 73.4% IV, $p = 0.0002$), while dinoflagellates increased at NH_4^+-enriched sites in Card Sound, Barnes Sound, and inshore sites in South-Central Bay (cluster C; 62.0% IV, $p = 0.0006$; Figs. 6, 7c, and 8; Supplemental Fig. 1).

Discussion

Despite its enormous size, strong winds, and close proximity to the southeast Florida coast, Hurricane Irma had a short-lasting (< 3-month) effect on water quality and phytoplankton communities in Biscayne Bay, which indicates that the bay is resilient to pulse disturbances. Large pre- and post-storm-related freshwater inflows increased nutrient loading into the bay, producing short-lived changes in phytoplankton

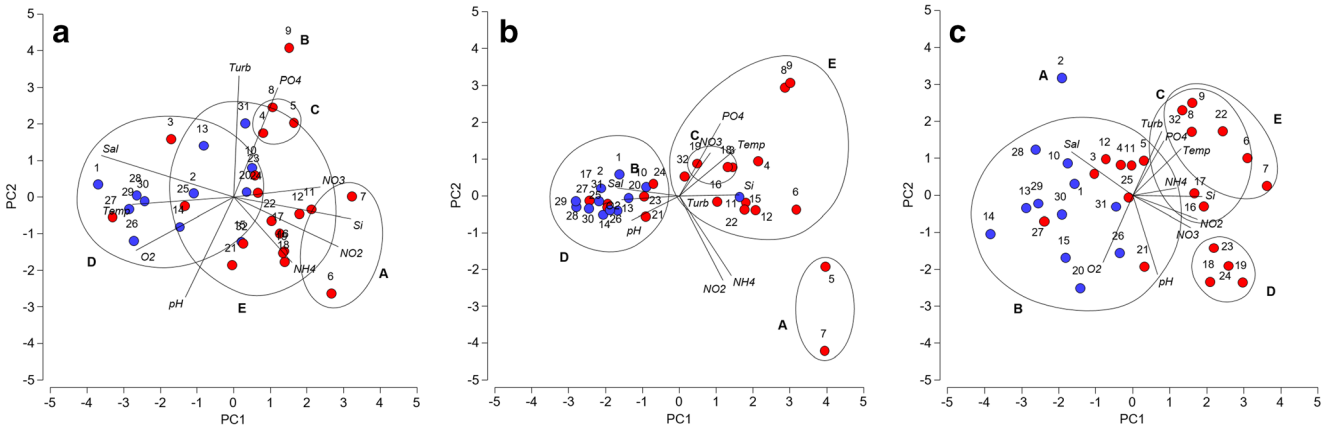

Fig. 5 Principal component ordination diagrams of sites based on Euclidean similarity in water quality in **a** September 2017, **b** November 2017, and **c** January 2018. Sites are coded by sampling locations (canals (red dots) vs. inshore (blue dots)), and clusters represent groups of sites with similar water quality. Arrows represent the direction and magnitude of correlation of environmental variables with principal components (PCs)

community structure, driven largely by decreases in diatoms and increases in cyanobacteria abundance, but relatively modest increases in total phytoplankton biomass.

The 2017 wet season was the wettest on record in South Florida since 1932, with several tropical storms, including Hurricane Irma, soaking and bringing water stages to record levels across the entire region (South Florida Water Management District 2018b). In preparation for Hurricane Irma, the SFWMD followed standard emergency operating procedures (USACE 2012) and opened the coastal structures along Biscayne Bay to lower the primary canal levels in preparation to receive discharge from the secondary canals that drain residential areas in Miami-Dade County. This increased discharges into the bay several days prior to arrival of the hurricane. During the event, the primary canal gates remained open in anticipation of losing electrical power, which would prevent the SFWMD from operating them remotely, and to prevent their failure, which could cause severe flooding of coastal areas. This allowed a surge of water to enter the canals causing backflow (negative flows), which was recorded at all Biscayne Bay coastal structures and was reflected in short-term, sharp S fluctuations at inshore locations. After the hurricane, storm surge and water drained from the mainland back to the bay in the form of amplified discharges via the coastal structures. Submarine groundwater discharges into the bay also likely increased, but the data are lacking for this time period. The large post-hurricane discharges and overland runoff resulted in large S fluctuations and a drop in average S across the entire inshore zone in the weeks following the event. This was especially pronounced in the south-central and southern parts of the bay, which experienced some of the largest post-hurricane canal discharges (Figs. 2b, c and 3). Increased freshwater inflows also increased nutrient loadings into the bay, as reflected in elevated concentrations of NO_x and NH_4^+ in the south-central part of the bay, PO_4^{3-} in northern and southern parts of the bay, and negative nutrient correlations with S (Figs. 4b-d; Table 2).

The south-central part of the bay is adjacent to the South Dade Agricultural Areas (SDAA), from which NO_x loads are substantially larger compared to urban areas in northern Miami-Dade County (Caccia and Boyer 2005, 2007; Zhang et al. 2009; Carey et al. 2011). Earlier studies showed that 74% of the annual NO_x loading in this region comes from the Mowry (C-103/S-20F) and Princeton (C-102/S-21A) canals (Caccia and Boyer 2007), and this was reflected in the highest NO_3^- concentrations within and large discharges from these canals during the post–Hurricane Irma September survey (especially in Mowry Canal). Agricultural activities in this region require application of NO_3^- and potassium-rich fertilizers, which easily percolate through porous limestone into the groundwater underneath the SDAA and the canals draining this region (Bradner et al. 2005; Caccia and Boyer 2007). Hurricane Irma–induced nutrient loading from farmlands might have been particularly high because the timing of the event coincided with the beginning of the growing season in South Miami-Dade County, when intense fertilization occurs to stimulate plant growth (FASS 1997). Other possible sources of NO_x and NH_4^+ to this region include South Dade Wastewater Treatment Plant (SDWWTP) and the Black Point Landfill (Swart et al. 2013). Power shortages after extreme events and flooding often introduce partially treated and raw sewage from treatment plants into coastal regions. For example, after the 1996 Hurricane Fran and Hurricane Bertha, sewage treatment plant and pump station power failures caused diversions of millions of liters of raw and partially treated human waste into Cape Fear River and Cape Fear Watershed (North Carolina). This was combined with overtopping of several swine waste lagoons by floodwater

Table 2 Spearman rank correlation coefficients for quantitative variables measured during September 2017, November 2017, and January 2018 surveys at 32 locations in Biscayne Bay. S = salinity (PSU), Temp = water temperature (°C), pH, SiO_2 = silica (μM), (NO_3^- = nitrate (μM), NO_2^- = nitrite (μM), NH_4^+ = ammonium (μM), PO_4^{3-} = orthophosphate (μM), O_2 = dissolved oxygen (mg/l), Turb = turbidity (NTU), chlA = chlorophyll *a* (μg/L)

Variables	S	Temp	pH	SiO_2	NO_2^-	NO_3^-	NH_4^+	PO_4^{3-}	O_2	Turb	chlA
September 2017											
S	1										
Temp	.593**	1									
pH	0.063	0.234	1								
SiO_2	−.784**	−.470**	−0.097	1							
NO_2^-	−.535**	−0.31	−0.044	0.265	1						
NO_3^-	−.458**	−0.202	−0.087	0.343	.620**	1					
NH_4^+	−0.209	−0.187	−0.154	0.063	.547**	−0.033	1				
PO_4^{3-}	0.059	−0.291	−0.226	−0.163	0.09	0.155	−0.046	1			
O_2	.482**	.399*	.573**	−.548**	−0.216	−0.31	−0.19	−0.197	1		
Turb	0.179	−0.05	−.404*	−0.124	−0.101	0.069	−0.286	.574**	−0.274	1	
chlA	0.249	0.07	0.15	−0.292	−0.042	−0.254	−0.05	0.086	0.067	0.111	1
November 2017											
S	1										
Temp	−.673**	1									
pH	.357*	−.502**	1								
SiO_2	−.952**	.743**	−.461**	1							
NO_2^-	−.472**	0.348	.0.138	.399*	1						
NO_3^-	−.688**	.644**	−0.217	.610**	.608**	1					
NH_4^+	−.666**	.595**	−.545**	.717**	.569**	.467**	1				
PO_4^{3-}	−.509**	.634**	−.635**	.483**	.401*	.540**	.571**	1			
O_2	.604**	−.697**	.639**	−.671**	−0.338	−0.293	−.612**	−.697**	1		
Turb	−0.251	0.067	0.087	0.229	−0.069	0.04	0.31	0.019	−0.068	1	
chlA	−.418*	−0.065	−0.134	.367*	0.166	0.001	.388*	0.051	−0.118	.528**	1
January 2018											
S	1										
Temp	−.434*	1									
pH	−.669**	−0.16	1								
SiO_2	−.718**	.504**	0.274	1							
NO_2^-	−.766**	.447*	.533**	.699**	1						
NO_3^-	−.695**	.506**	0.293	.850**	.752**	1					
NH_4^+	−.583**	0.253	.413*	.633**	.657**	.400*	1				
PO_4^{3-}	0.03	.573**	−.511**	0.348	−0.028	0.217	0.161	1			
O_2	−0.067	−.432**	.446*	−.396*	−0.057	−0.068	−.393*	−.713**	1		
Turb	−0.134	.420*	−0.129	0.324	.441*	0.245	.470**	0.347	.450**	1	
chlA	−0.176	.561**	−0.324	.442*	.425*	.401*	0.306	.462**	−.421*	.628**	1

* Correlation is significant at the 0.05 level

** Correlation is significant at the 0.01 level

and discharging large quantities of concentrated organic waste into the river, resulting in eutrophication and hypoxia (Mallin et al. 1999). Similarly, sewage spills were also reported into Biscayne Bay after Hurricane Irma (Florida Department of Environmental Protection 2018). Canals near Black Point, where the SDWWTP and landfill are located, had the highest concentrations of NH_4^+ after the hurricane. The northern part of the bay (north of Virginia Key), which is adjacent to highly populated Miami metropolitan areas, receives high NH_4^+ and PO_4^{3-} loadings (~ 74% and ~ 60% of the total annual loading to the bay, respectively) from the Miami River (C6), Little River (C7), and Snake Creek (C9) canals (Caccia and Boyer

Table 3 Factor loadings for five principal components

Variables	PC1	PC2	PC3	PC4	PC5
September 2017					
S	*− 0.477*	0.189	− 0.125	0.132	0.003
Temp	− 0.365	− 0.033	− 0.248	− 0.098	*0.768*
pH	− 0.174	*− 0.454*	− 0.008	− 0.447	− 0.295
SiO_2	*0.422*	− 0.097	0.375	− 0.190	0.169
NO_2^-	0.376	− 0.226	*− 0.527*	0.097	0.032
NO_3^-	0.312	0.045	− 0.402	*− 0.539*	0.233
NH_4^+	0.209	− 0.297	− 0.311	*0.629*	0.001
PO_4^{3-}	0.158	*0.497*	− 0.296	− 0.138	− 0.329
O_2	− 0.351	− 0.240	*− 0.367*	− 0.147	− 0.361
Turb	0.018	*0.550*	− 0.157	0.031	− 0.035
November 2017					
S	*− 0.404*	0.049	− 0.324	0.144	− 0.230
Temp	*0.367*	0.304	− 0.035	0.045	0.250
pH	− 0.310	− 0.162	0.369	− 0.179	*0.467*
SiO_2	*0.392*	0.004	0.332	0.051	0.344
NO_2^-	0.286	*− 0.551*	− 0.166	− 0.231	− 0.214
NO_3^-	0.201	0.281	0.357	*− 0.622*	− 0.348
NH_4^+	0.341	*− 0.521*	− 0.066	− 0.004	− 0.178
PO_4^{3-}	0.266	*0.473*	− 0.285	− 0.026	− 0.235
O_2	− 0.376	− 0.024	0.217	*− 0.384*	− 0.258
Turb	0.036	− 0.002	*0.600*	0.594	− 0.477
January 2018					
S	*− 0.398*	0.282	− 0.075	0.225	− 0.125
Temp	0.316	0.302	0.235	− 0.314	*0.485*
pH	0.159	*− 0.517*	− 0.195	0.182	0.431
SiO_2	*0.452*	− 0.009	0.106	0.257	− 0.222
NO_2^-	*0.420*	− 0.157	− 0.134	− 0.318	0.065
NO_3^-	0.375	− 0.211	0.285	0.044	*− 0.402*
NH_4^+	0.284	0.047	*− 0.553*	0.401	− 0.241
PO_4^{3-}	0.201	0.354	*0.531*	0.396	0.008
O_2	− 0.194	*− 0.436*	0.323	− 0.303	− 0.422
Turb	0.189	0.418	− 0.314	*− 0.488*	− 0.336

Loadings are the Spearman correlation between the ranked data with the principal components. In total, the first two principal components explained 54.3%, 61.0%, and 63.8% of the variation in the original September 2017, November 2017, and January 2018 data

2007). The post-hurricane surveys also revealed consistently elevated PO_4^{3-} and NH_4^+ concentrations in the Coral Gables Canal (C3). Many houses in this area, and ~21% in the entire Miami Dade County, are still on septic tanks, which back up and overflow during periods of extreme precipitation, when groundwater levels rapidly increase (Florida Department of Environmental Protection 2018), adding to the nutrient load.

Biscayne Bay is normally a total phosphorus (TP)-limited system, especially the south-central part of the bay (Caccia and Boyer 2007; Zhang et al. 2009) which received an excess of NO_x from the farmlands after the hurricane. Low phosphorus (PO_4^{3-}) concentration limits phytoplankton growth in the bay, which is reflected in historically lower phytoplankton biomass compared to other Florida estuarine systems with less severe nutrient limitations (Boyer et al. 2009; Briceño et al. 2013). Increased nutrient loading after Hurricane Irma stimulated phytoplankton growth in Biscayne Bay, which is a common occurrence in estuarine systems after hurricanes (Hagy et al. 2006; Zhao et al. 2008; Zhang et al. 2009; Peierls et al. 2003; Wetz and Paerl 2008; Paerl et al. 2018). For example, passage of three sequential hurricanes over Pamlico Sound (North Carolina) in the fall of 1999 briefly increased inorganic nitrogen (NO_x, NH_4^+) and PO_4^{3-} concentrations (by 2–3 times) during the flooding, which subsequently increased algal biomass until late spring of 2000 (Peierls et al. 2003). Similarly, increased nutrient loadings into Chesapeake Bay (Maryland and Virginia) after Hurricane Isabel in September 2003 resulted in a twofold increase in algal biomass in the mid- and lower parts of the bay, with an abrupt return to long-term average chl *a* concentration by early October (Miller et al. 2006). The post–Hurricane Irma ephemeral eutrophication of Biscayne Bay stimulated phytoplankton growth in secluded inshore areas of the northern and southern parts of the bay, but the biomass gradually decreased over time (except for northern part of the bay, where elevated algal biomass might not be an exclusively hurricane-related phenomenon). Large freshwater inputs from point sources (e.g., rivers, creeks, canals) following extreme weather events prevent algal biomass from accumulating near the point source discharges due to high flushing and instead stimulate biomass in more downstream locations (Miller et al. 2006; Peierls et al. 2003; Paerl et al. 2006, 2018). This was reflected in lower algal biomass in the Miami-Dade canals compared to inshore locations in September. As nutrient concentrations at inshore locations became depleted and freshwater discharges from the canals declined, algal biomass peaks shifted to nutrient-enriched, warmer waters in the canals from the inshore sites.

The mechanisms driving phytoplankton community composition are difficult to distinguish, but it is clear that Hurricane Irma–related nutrient enrichment and significant changes in physical water quality parameters had a profound effect on both phytoplankton biomass and community structure patterns. The relative contribution of cyanobacteria to the total chl *a* pool was largest in September and declined over time in favor of diatoms. The highest concentrations of cyanobacteria were recorded in the southern and north-central parts of the bay, at sites with elevated NH_4^+ concentrations and NH_4^+/NO_3^- ratios (Figs. 4b and 8). NH_4^+ is a preferred nitrogen form by this phytoplankton group because it is the least energy-demanding N source for cells to assimilate (Lomas and Glibert 1999; Glibert et al. 2016, Glibert and Burford 2017; Shangguan et al. 2017a, 2017b). Mesocosm experiments in tidal estuarine systems showed that NH_4^+ enrichment with respect to NO_3^-

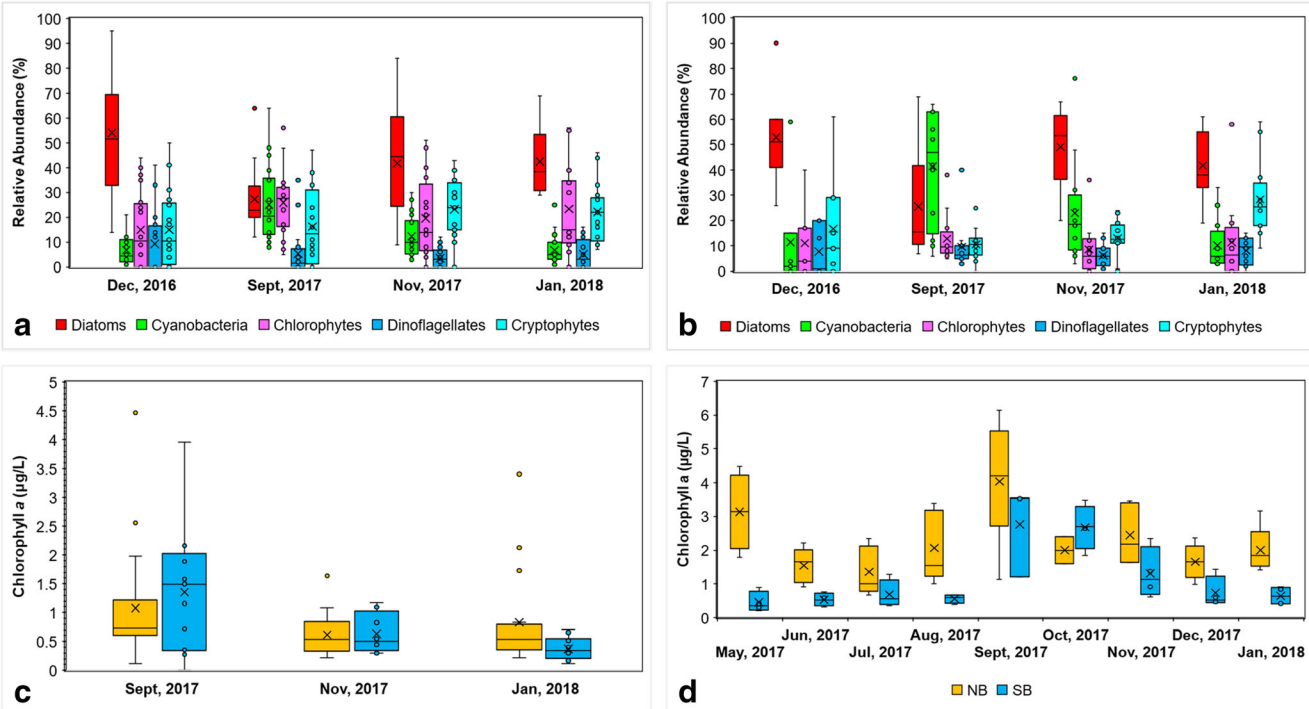

Fig. 6 Temporal differences in relative abundance of diatoms, cyanobacteria, chlorophytes, dinoflagellates, and cryptophytes at 32: **a** canal and **b** inshore locations among December 2016, September 2017, November 2017, and January 2018 surveys; **c** algal biomass (chl *a*) at 32 canal (yellow) and inshore (blue) locations among September 2017, November 2017, and January 2018 surveys; and **d** northern (NB) and southern (SB) Biscayne Bay among May–December 2017 and January 2018 surveys. The box shows the interquartile range (1st–3rd quartiles). The left "whisker" represents the smallest number in the set, and the far right "whisker" represents the largest number in the set. The median is represented by a vertical bar in the center of the box and mean by an "x" symbol within the box

promotes growth of cyanobacteria (Domingues et al. 2011; Shangguan et al. 2017b). The southern part of Biscayne Bay is an area of frequent picocyanobacteria blooms following extreme weather events, which result in large internal and external pulses of nutrients. The largest and longest-lasting bloom of this kind in this region was recorded between 2005 and 2008 (Rudnick et al. 2007; Glibert et al. 2009). This bloom developed after passage of three hurricanes in 2005 (Katrina, Rita, and Wilma) and a major roadway construction and mangrove soil excavation in the Florida Keys, which resulted in significant external (from the mainland) and internal (from soil) nutrient loading into southern Biscayne Bay and northeast Florida Bay (Rudnick et al. 2007; Glibert et al. 2009). Picocyanos such as *Synechococcus* sp., which is the bloom forming species in southern Biscayne Bay and northeastern Florida Bay (Phlips and Badylak 1996; Rudnick et al. 2007; Glibert et al. 2009), are good competitors in warm (> 25 °C), TP-limited ecosystems (Irwin et al. 2006; Reynolds 2006; Finkel et al. 2009), like South Florida estuaries. Because of the scarcity of phytoplankton studies in northern Biscayne Bay, it is currently unclear whether cyanobacteria commonly and frequently dominate phytoplankton communities in this region after extreme weather events. Diatoms are typically NO_3^- opportunists and require SiO_2 to build their valves (Lomas and Glibert 2000; Glibert et al. 2016; Glibert and Burford 2017; Shangguan et al. 2017a, 2017b). This phytoplankton group was most abundant at NO_3^-- and SiO_2-enriched sites in the south-central part of the bay and the canals. Chlorophytes were very abundant in P- and N-enriched Coral Gables and Snapper Creek canals, which intersect highly populated old Miami neighborhoods with aging urban infrastructure and leaky septic tanks. In general, chlorophytes are often associated with shallow, nutrient-rich freshwater environments, particularly those characterized by elevated PO_4^{3-} concentrations and high light penetration (Barica et al. 1980; Jensen et al. 1994). They are competitive with other phytoplankton in freshwater environments due to high growth rates and diverse mechanisms of N assimilation (Fernandez and Galvan 2007). Changes in spatial-temporal phytoplankton community structure in the months following Hurricane Irma reflect the annual T patterns in South Florida, with a secondary influence from the hurricane-related perturbations.

Conclusions

Continuous urban development along the southeast Florida coast weakens the resilience of the region's estuarine

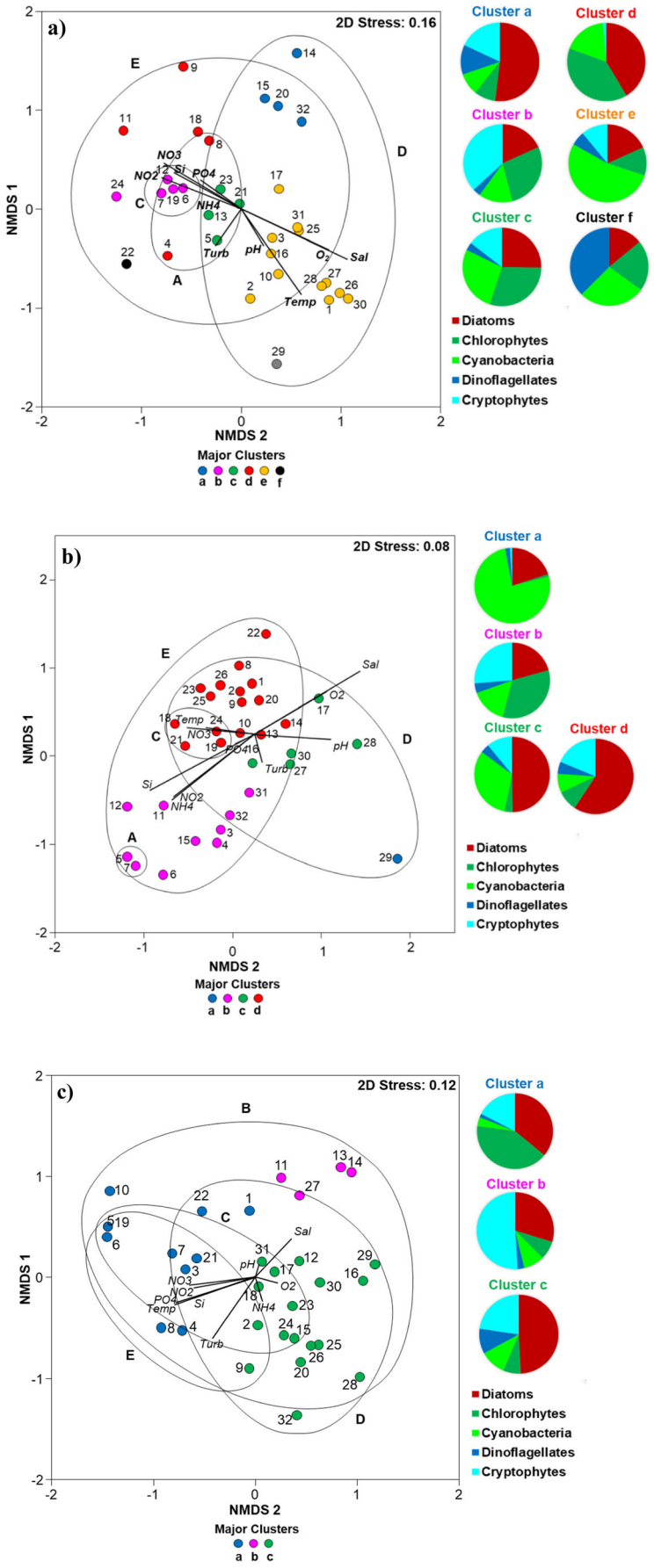

Fig. 7 Nonmetric multidimensional scaling ordination diagrams of sites based on Bray-Curtis similarity in phytoplankton community structure in **a** September 2017, **b** November 2017, and **c** January 2018. Sites are color-coded by clusters representing groups of sites with a similar phytoplankton community structure. Water quality clusters (circles) are superimposed on phytoplankton clusters. Arrows represent the direction and magnitude of correlation of environmental variables with phytoplankton community compositional differences

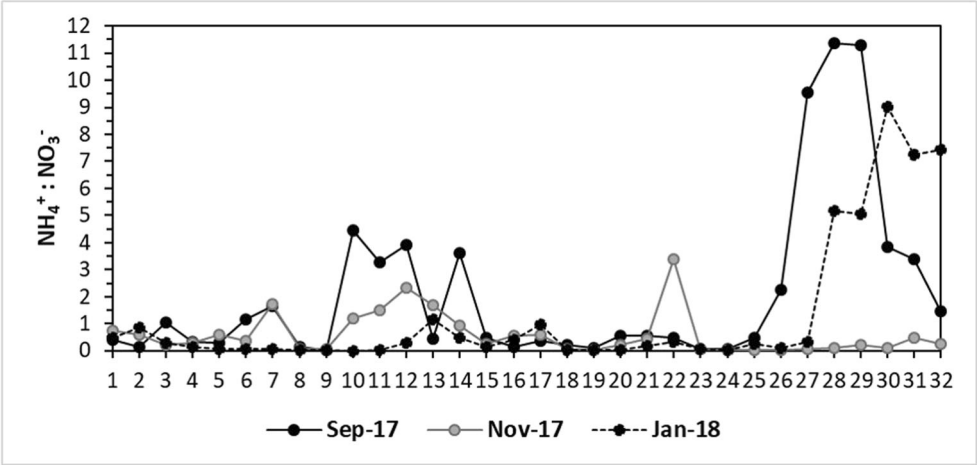

Fig. 8 Changes in NH_4^+/NO_3^- ratio at 32 SFWMD/NOAA inshore and canal locations in Biscayne Bay

systems and their biota to withstand severe fluctuations in hydrodynamic and water quality processes within the estuaries caused by natural pressures. Our study showed that Biscayne Bay is still resilient to pulse disturbances like hurricanes. Although the bay experienced record amounts of pre– and post–Hurricane Irma freshwater inflows and nutrient loads, water quality and phytoplankton dynamics returned quickly (< 3 months) to pre-disturbance state, which was also observed after Hurricane Katrina in 2005 (Zhang et al. 2009). However, the resilience of the structural components of Biscayne Bay ecosystem (e.g., seagrasses, corals, sponges) to hurricanes is poorly understood. Also, the fate and impacts of terrigenous organic material (e.g., colored dissolved organic matter) transported from marshes and wetlands and marine sources of organic material (e.g., uprooted submersed aquatic vegetation) deposited at inshore locations on the Biscayne Bay ecosystem (e.g., benthic habitats and water quality) are unclear. These topics should be better investigated following extreme weather events in the future.

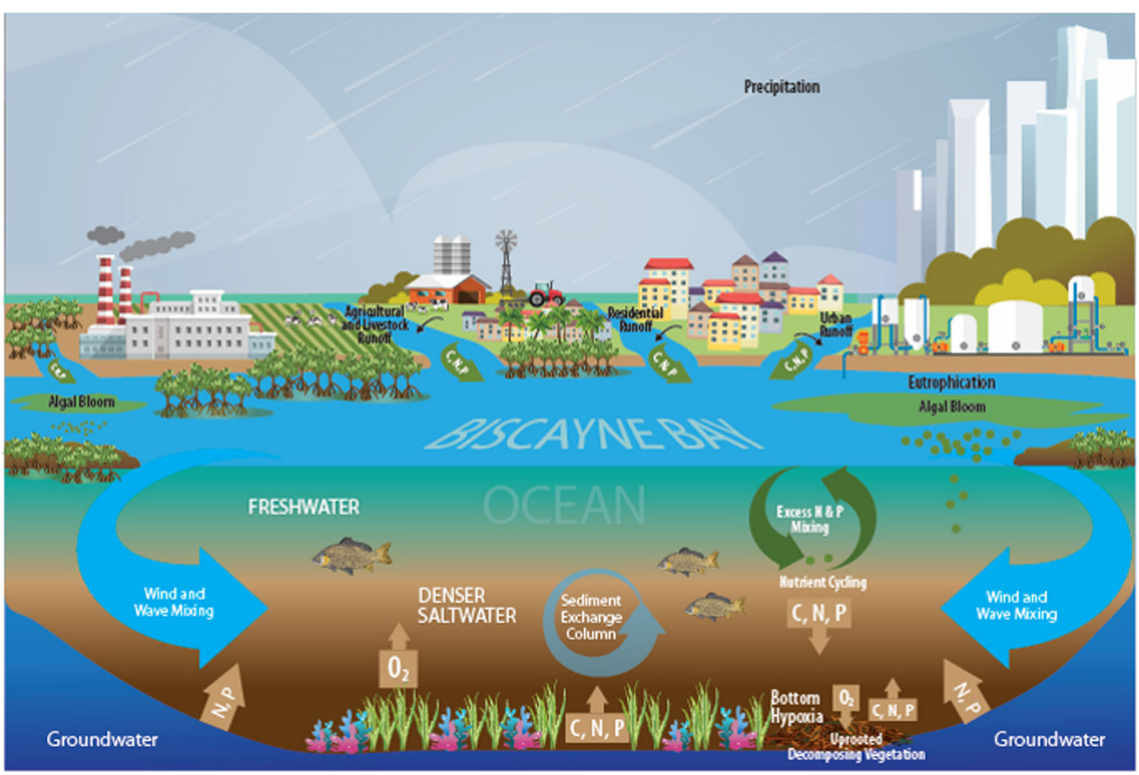

Fig. 9 Conceptual diagram of post-hurricane conditions in Biscayne Bay. The diagram shows different sources of nutrients, the establishment of hypoxia due to strong water stratification and decomposition of organic material at inshore locations and the canals, and eutrophication due to nutrient enrichment in the southern and northern parts of Biscayne Bay

Increased sampling frequency and supplementary sampling after hurricanes and other extreme weather events are recommended to better understand responses of the South Florida estuarine systems to possible future increases in the frequency and magnitude of hurricanes and extreme precipitation events (IPCC 2018). Understanding how estuaries respond to and recover from such severe events is of fundamental significance for environmental assessment and management of these systems.

Acknowledgments This study was made possible thanks to the collaboration between South Florida Water Management District, the NOAA Fisheries Southeast Fisheries Science Center, and the NOAA Research Atlantic Oceanographic and Meteorological Laboratory. The study grew out of an earlier collaboration between Florida International University, NOAA, the National Research Council (Fellowship), and the NOAA Biscayne Bay Habitat Focus Area Initiative, as supported by the NOAA Fisheries Offices of Habitat Conservation and Science and Technology and by the NOAA Fisheries Southeast Regional Office. Many thanks are due to NOAA, DERM, and BNP technicians for post–Hurricane Irma field assistance and Biscayne Bay water quality monitoring. We would also like to thank Ellen Negley from SFWMD Creative Services for her help with the graphics, and internal (SFWMD and NOAA) and external (Estuaries and Coasts) reviewers for detailed and helpful comments on the manuscript.

References

Anderson, M.J. 2001. Permutation tests for univariate or multivariate analysis of variance and regression. *Canadian Journal of Fisheries and Aquatic Sciences* 58 (3): 626–639.

Anderson, M.J. 2014. Permutational multivariate analysis of variance (PERMANOVA). In *Wiley StatsRef: Statistics Reference Online*, 1–15.

Barica, J., H. Kling, and J. Gibson. 1980. Experimental manipulation of algal bloom composition by nitrogen addition. *Canadian Journal of Fisheries and Aquatic Sciences* 37 (7): 1175–1183.

Bianucci, L., K. Balaguru, R.W. Smith, L.R. Leung, and J.M. Moriarty. 2018. Contribution of hurricane-induced sediment resuspension to coastal oxygen dynamics. *Scientific Reports* 8 (1): 15740.

Boyer, J.N., C.R. Kelble, P.B. Ortner, and D.T. Rudnick. 2009. Phytoplankton bloom status: Chlorophyll a biomass as an indicator of water quality condition in the southern estuaries of Florida, USA. *Ecological Indicators* 9 (6): S56–S67.

Bradner, A., B.F. McPherson, R.L. Miller, G. Kish, and B. Bernard. 2005. *Quality of ground water in the Biscayne Aquifer in Miami-Dade, Broward, and Palm Beach counties, Florida, 1996–1998, with emphasis on contaminants (no. OPEN-FILE-2004-1438)*. Washington DC: United States Geological Survey.

Bray, J.R., and J.T. Curtis. 1957. An ordination of the upland forest communities of southern Wisconsin. *Ecological Monographs* 27 (4): 325–349.

Briceño, H.O., J.N. Boyer, J. Castro, and P. Harlem. 2013. Biogeochemical classification of South Florida's estuarine and coastal waters. *Marine Pollution Bulletin* 75 (1–2): 187–204.

Caccia, V.G., and J.N. Boyer. 2005. Spatial patterning of water quality in Biscayne Bay, Florida as a function of land use and water management. *Marine Pollution Bulletin* 50 (11): 1416–1429.

Caccia, V.G., and J.N. Boyer. 2007. A nutrient loading budget for Biscayne Bay, Florida. *Marine Pollution Bulletin* 54 (7): 994–1008.

Cangialosi, J. P., Latto, A. S., and Berg, R. 2018. *National Hurricane Center tropical cyclone report: Hurricane Irma*. National Oceanic and Atmospheric Administration: May, 30.

Carey, R.O., K.W. Migliaccio, Y. Li, B. Schaffer, G.A. Kiker, and M.T. Brown. 2011. Land use disturbance indicators and water quality variability in the Biscayne Bay watershed, Florida. *Ecological Indicators* 11 (5): 1093–1104.

Clarke, K.R. 1993. Non-parametric multivariate analyses of changes in community structure. *Australian Journal of Ecology* 18 (1): 117–143.

Clarke, K.R., and R.N. Gorley. 2015. *Getting started with PRIMER v7*. Plymouth: PRIMER-E.

Clarke, K.R., R.N. Gorley, P.J. Somerfield, and R.M. Warwick. 2014. *Change in marine communities: an approach to statistical analysis and interpretation*. 3rd ed. Plymouth: PRIMER-E.

Domingues, R.B., T.P. Anselmo, A.B. Barbosa, U. Sommer, and H.M. Galvão. 2011. Light as a driver of phytoplankton growth and production in the freshwater tidal zone of a turbid estuary. *Estuarine, Coastal and Shelf Science* 91 (4): 526–535.

Dufrêne, M., and P. Legendre. 1997. Species assemblages and indicator species: the need for a flexible asymmetrical approach. *Ecological Monographs* 67 (3): 345–366.

Dunn, O.J. 1964. Multiple comparisons using rank sums. *Technometrics* 6 (3): 241–252.

FASS 1997. *Florida agricultural statistics: vegetable summary (1995–96)*. Florida Agricultural Statistics Service, Florida Department of Agriculture and Consumer Services, 70 pp.

Fernandez, E., and A. Galvan. 2007. Inorganic nitrogen assimilation in Chlamydomonas. *Journal of Experimental Botany* 58 (9): 2279–2287.

Finkel, Z.V., J. Beardall, K.J. Flynn, A. Quigg, T.A.V. Rees, and J.A. Raven. 2009. Phytoplankton in a changing world: cell size and elemental stoichiometry. *Journal of Plankton Research* 32 (1): 119–137.

Florida Department of Environmental Protection. 2018. Notices of Pollution. http://prodenv.dep.state.fl.us/DepPNP/reports/viewIncidentDetails?page=1. Accessed 10 September 2018.

Glibert, P.M., and M.A. Burford. 2017. Globally changing nutrient loads and harmful algal blooms: recent advances, new paradigms, and continuing challenges. *Oceanography* 30 (1): 58–69.

Glibert, P.M., C.A. Heil, D.T. Rudnick, C.J. Madden, J.N. Boyer, and S. Kelly. 2009. Florida Bay: water quality status and trends, historic and emerging algal bloom problems. *Contributions in Marine Science* 38: 5–17.

Glibert, P.M., F.P. Wilkerson, R.C. Dugdale, J.A. Raven, C.L. Dupont, P.R. Leavitt, et al. 2016. Pluses and minuses of ammonium and nitrate uptake and assimilation by phytoplankton and implications for productivity and community composition, with emphasis on nitrogen-enriched conditions. *Limnology and Oceanography* 61 (1): 165–197.

Grant, C.S., and J.W. Louda. 2010. Microalgal pigment ratios in relation to light intensity: implications for chemotaxonomy. *Aquatic Biology* 11 (2): 127–138.

Hagerthey, S.E., J.W. Louda, and P. Mongkronsri. 2006. Evaluation of pigment extraction methods and a recommended protocol for periphyton chlorophyll *a* determination and chemotaxonomic assessment. *Journal of Phycology* 42 (5): 1125–1136.

Hagy, J.D., J.C. Lehrter, and M.C. Murrell. 2006. Effects of hurricane Ivan on water quality in Pensacola Bay, Florida. *Estuaries and Coasts* 29 (6): 919–925.

IPCC (2018). Global warming of 1.5°C. An IPCC special report on the impacts of global warming of 1.5°C above pre-industrial levels and related global greenhouse gas emission pathways, in the context of strengthening the global response to the threat of climate change, sustainable development, and efforts to eradicate poverty [V. Masson-Delmotte, P. Zhai, H. O. Pörtner, D. Roberts, J. Skea, P.R.

Shukla, A. Pirani, W. Moufouma-Okia, C. Péan, R. Pidcock, S. Connors, J. B. R. Matthews, Y. Chen, X. Zhou, M. I. Gomis, E. Lonnoy, T. Maycock, M. Tignor, T. Waterfield (eds.)]. In Press.

Irwin, A.J., Z.V. Finkel, O.M. Schofield, and P.G. Falkowski. 2006. Scaling-up from nutrient physiology to the size-structure of phytoplankton communities. *Journal of Plankton Research* 28 (5): 459–471.

Jensen, J.P., E. Jeppesen, K. Olrik, and P. Kristensen. 1994. Impact of nutrients and physical factors on the shift from cyanobacterial to chlorophyte dominance in shallow Danish lakes. *Canadian Journal of Fisheries and Aquatic Sciences* 51 (8): 1692–1699.

Jolliffe, I. 2011. Principal component analysis. In *International encyclopedia of statistical science*, 1094–1096. Berlin, Heidelberg: Springer.

Kruskal, W.H., and W.A. Wallis. 1952. Use of ranks in one-criterion variance analysis. *Journal of the American Statistical Association* 47 (260): 583–621.

Kruskal, J. B., and M. Wish. 1978. Multidimensional scaling. In Sage University Paper Series on Quantitative Applications in the Social Sciences, No. 07-011, Sage Publications, Newbury Park. https://doi.org/10.4135/9781412985130.

Langevin, C.D. 2003. Simulation of submarine ground water discharge to a marine estuary: Biscayne Bay, Florida. *Groundwater* 41 (6): 758–771.

Liu, X., M. Wang, and W. Shi. 2009. A study of a Hurricane Katrina–induced phytoplankton bloom using satellite observations and model simulations. *Journal of Geophysical Research, Oceans* (C3): 114.

Lomas, M. W., and Glibert, P. M. 1999. Temperature regulation of nitrate uptake: A novel hypothesis about nitrate uptake and reduction in coolwater diatoms. *Limnology and Oceanography* 44(3):556–572.

Lomas, M.W., and P.M. Glibert. 2000. Comparisons of nitrate uptake, storage, and reduction in marine diatoms and flagellates. *Journal of Phycology* 36 (5): 903–913.

Louda, J.W., J. Li, L. Liu, M.N. Winfree, and E.W. Baker. 1998. Chlorophyll-a degradation during cellular senescence and death. *Organic Geochemistry* 29 (5–7): 1233–1251.

Mallin, M.A., and C.A. Corbett. 2006. How hurricane attributes determine the extent of environmental effects: multiple hurricanes and different coastal systems. *Estuaries and Coasts* 29 (6): 1046–1061.

Mallin, M.A., M.H. Posey, G.C. Shank, M.R. McIver, S.H. Ensign, and T.D. Alphin. 1999. Hurricane effects on water quality and benthos in the Cape Fear watershed: natural and anthropogenic impacts. *Ecological Applications* 9 (1): 350–362.

Massie, J.A., B. Strickland, R.O. Santos, J. Hernandez, N. Viadero, H. Willoughby, M. Heithaus, and J.S. Rehage. this volume. Going down the river: hurricane driven movements of Common Snook in response to falling barometric pressure and increasing stage in a subtropical coastal river. *Estuaries and Coasts*.

McCune, B., J.B. Grace, and D.L. Urban. 2002. *Analysis of ecological communities*. Vol. 28. Gleneden Beach: MjM software design.

Miller, W.D., L.W. Harding Jr., and J.E. Adolf. 2006. Hurricane Isabel generated an unusual fall bloom in Chesapeake Bay. *Geophysical Research Letters* 33 (6).

Munroe, D., A. Tabatabai, I. Burt, D. Bushek, E.N. Powell, and J. Wilkin. 2013. Oyster mortality in Delaware Bay: impacts and recovery from Hurricane Irene and Tropical Storm Lee. *Estuarine, Coastal and Shelf Science* 135: 209–219.

NEXRAD. 2018. SFWMD Rainfall Estimates Database http://apps.sfwmd.gov/nexrad2/nrdmain.action. Accessed 10 September 2018.

NOAA. 2018. NOAA Tides and Currents Database. https://tidesandcurrents.noaa.gov/stationhome.html?id=8723214. Accessed 10 September 2018.

Paerl, H.W., J.D. Bales, L.W. Ausley, C.P. Buzzelli, L.B. Crowder, L.A. Eby, et al. 2001. Ecosystem impacts of three sequential hurricanes (Dennis, Floyd, and Irene) on the United States' largest lagoonal estuary, Pamlico Sound, NC. *Proceedings of the National Academy of Sciences* 98 (10): 5655–5660.

Paerl, H.W., L.M. Valdes, A.R. Joyner, B.L. Peierls, M.F. Piehler, S.R. Riggs, et al. 2006. Ecological response to hurricane events in the Pamlico Sound system, North Carolina, and implications for assessment and management in a regime of increased frequency. *Estuaries and Coasts* 29 (6): 1033–1045.

Paerl, H.W., J.R. Crosswell, B. Van Dam, N.S. Hall, K.L. Rossignol, C.L. Osburn, et al. 2018. Two decades of tropical cyclone impacts on North Carolina's estuarine carbon, nutrient and phytoplankton dynamics: implications for biogeochemical cycling and water quality in a stormier world. *Biogeochemistry* 141 (3): 307–332.

Peierls, B.L., R.R. Christian, and H.W. Paerl. 2003. Water quality and phytoplankton as indicators of hurricane impacts on a large estuarine ecosystem. *Estuaries and Coasts* 26 (5): 1329–1343.

Phlips, E.J., and S. Badylak. 1996. Spatial variability in phytoplankton standing crop and composition in a shallow inner-shelf lagoon, Florida Bay, Florida. *Bulletin of Marine Science* 58 (1): 203–216.

Powell, M.D., S.H. Houston, and T.A. Reinhold. 1996. Hurricane Andrew's Landfall in South Florida, part I: Standardizing measurements for documentation of surface wind fields. *Weather and Forecasting* 11: 329–349.

Radabaugh, K.R., Moyer, R.P., Chappel, A.R., Dontis, E.E., Russo, C.E., Joyse. K.M., Bownik, M.W., Goeckner, A.H., Khan, N.S. 2019. Mangrove damage, delayed mortality, and early recovery following Hurricane Irma at two landfall sites in southwest Florida, USA. https://doi.org/10.1007/s12237-019-00564-8.

Reynolds, C.S. 2006. *The ecology of phytoplankton*. Cambridge, New York: Cambridge University Press.

Rudnick, D., C. Madden, S. Kelly, J. Boyer, S. Blair, K. Cunniff, and C. Kelble. 2007. Disturbance and ecosystem change in Florida Bay and southern Biscayne Bay. In *Providence: Estuarine Research Federation Conference*.

Shangguan, Y., P.M. Glibert, J.A. Alexander, C.J. Madden, and S. Murasko. 2017a. Nutrients and phytoplankton in semienclosed lagoon systems in Florida Bay and their responses to changes in flow from Everglades restoration. *Limnology and Oceanography* 62 (S1): S327–S347.

Shangguan, Y., P.M. Glibert, J. Alexander, C.J. Madden, and S. Murasko. 2017b. Phytoplankton assemblage response to changing nutrients in Florida Bay: results of mesocosm studies. *Journal of Experimental Marine Biology and Ecology* 494: 38–53.

South Florida Water Management District. 2015. Atlas of flow computations at hydraulic structures in the South Florida Water Management District. Technical Publication #2015-001, pp. 154.

South Florida Water Management District. 2018a. SFWMD DBHYDRO Database. https://www.sfwmd.gov/science-data/dbhydro. Accessed 10 September 2018.

South Florida Water Management District. 2018b. SFWMD Weather Data. https://www.sfwmd.gov/weather-radar/rainfall-historical/normal. Accessed 10 September 2018.

Stalker, J.C., R.M. Price, and P.K. Swart. 2009. Determining spatial and temporal inputs of freshwater, including submarine groundwater discharge, to a subtropical estuary using geochemical tracers, Biscayne Bay, South Florida. *Estuaries and Coasts* 32 (4): 694–708.

Stevens, P.W., D.A. Blewett, and J.P. Casey. 2006. Short-term effects of a low dissolved oxygen event on estuarine fish assemblages following the passage of Hurricane Charley. *Estuaries and Coasts* 29 (6): 997–1003.

Steward, J.S., R.W. Virnstein, M.A. Lasi, L.J. Morris, J.D. Miller, L.M. Hall, and W.A. Tweedale. 2006. The impacts of the 2004 hurricanes on hydrology, water quality, and seagrass in the central Indian River Lagoon, Florida. *Estuaries and Coasts* 29 (6): 954–965.

Strickland, B., J. Massie, N. Viadero, J. Hernandez, R. Santos, V. Paz, K.R. Gastrich, P. O'Donnell, A. Kroetz, D.T. Ho, H. Willoughby, J.S. Rehage, and M.R. Heithaus. Movements of juvenile bull sharks

in response to a major hurricane within tropical estuarine nursery area. (this volume).

Swart, P.K., W.T. Anderson, M.A. Altabet, C. Drayer, and S. Bellmund. 2013. Sources of dissolved inorganic nitrogen in a coastal lagoon adjacent to a major metropolitan area, Miami Florida (USA). *Applied Geochemistry* 38: 134–146.

Tomasko, D.A., C. Anastasiou, and C. Kovach. 2006. Dissolved oxygen dynamics in Charlotte Harbor and its contributing watershed, in response to Hurricanes Charley, Frances, and Jeanne—impacts and recovery. *Estuaries and Coasts* 29 (6): 932–938.

USACE. 2012. Water control plan for water conservation areas, Everglades National Park, and ENP-South Dade Conveyance System. pp. 137.

Wetz, M.S., and H.W. Paerl. 2008. Estuarine phytoplankton responses to hurricanes and tropical storms with different characteristics (trajectory, rainfall, winds). *Estuaries and Coasts* 31 (2): 419–429.

Wilson, S.S., B.T. Furman, M.O. Hall, and J.W. Fourqurean. Assessment of Hurricane Irma impacts on South Florida seagrass communities using long-term monitoring programs. (this volume).

Wingard, G.L., Bergstresser, S.E., Stackhouse, B.L., Jones, M.C., Marot, M.E., Daniels, A., Keller, K. This volume. This volume. Impacts of Hurricane Irma on Florida Bay islands, Everglades National Park.

Woodley, J.D., E.A. Chornesky, P.A. Clifford, J.B.C. Jackson, L.S. Kaufman, N. Knowlton, et al. 1981. Hurricane Allen's impact on Jamaican coral reefs. *Science* 214 (4522): 749–755.

Zhang, K., D. Whitman, S. Leatherman, and W. Robertson. 2005. Quantification of beach changes caused by Hurricane Floyd along Florida's Atlantic coast using airborne laser surveys. *Journal of Coastal Research* 211: 123–134.

Zhang, J.Z., C.R. Kelble, C.J. Fischer, and L. Moore. 2009. Hurricane Katrina induced nutrient runoff from an agricultural area to coastal waters in Biscayne Bay, Florida. *Estuarine, Coastal and Shelf Science* 84 (2): 209–218.

Zhao, H., D. Tang, and Y. Wang. 2008. Comparison of phytoplankton blooms triggered by two typhoons with different intensities and translation speeds in the South China Sea. *Marine Ecology Progress Series* 365: 57–65.

Zink, I.C., J. Browder, and C. Kelble. Extreme hurricane disturbance mediated shifts of a subtropical seagrass associated fish and macroinvertebrate community. (this volume).